JOURNAL OF APPLIED ELECTROCHEMISTRY 20 (1990) 740–748

Flow-through and flow-by porous electrodes of nickel foam
Part III: theoretical electrode potential distribution in the flow-by configuration

S. LANGLOIS, F. COEURET

Laboratoire de Génie des Procédés, CNRS-ENSCR, Avenue du Général Leclerc, 35700 Rennes Beaulieu, France

Received 27 April 1989; revised 20 November 1989

This paper deals with the theoretical potential distribution within a flow-by parallelepipedic porous electrode operating in limiting current conditions in a two-compartment electrolytic cell. The model takes into account the influence of the counter-electrode polarization and of the separator ohmic resistance. The results show that the design of the porous electrode requires the knowledge of the solution potential distribution within the whole cell volume.

Nomenclature

a_e specific surface area per unit volume of electrode
C_0 entrance concentration ($y = 0$)
C_s exit concentration ($y = y_0$)
E electrode potential ($= \phi_M - \phi_S$)
E_0 equilibrium electrode potential
F Faraday number
i current density
$\bar{k}_d$ mean mass transfer coefficient
K parameter $[a_{ea} zFi_{oa}/(\gamma_a RT)]^{1/2}$
L porous electrode thickness
n number of terms in Fourier serials
P specific productivity
Q_v volumetric flow-rate
$\bar{u}$ mean flow velocity based on empty channel
V constant potential
V_R electrode volume
x thickness variable
X conversion
y length variable
y_0 porous electrode length
z number of electrons in the electrochemical reaction

Greek symbols
α parameter $[= zF\bar{k}_d a_e C_0/\gamma_c]$
β parameter $[= \bar{k}_d a_e/\bar{u}]$
γ ionic electrolyte conductivity in pores
ϕ_S solution potential
ϕ_M matrix potential (ϕ_M = constant)
λ parameter $[= n\pi/y_0]$
μ parameter $[= \lambda + K]$
η overpotential

Suffices
a anodic
c cathodic
eq equilibrium
s separator
S solution

1. Introduction

The flow-by configuration of porous electrodes is known to be more adapted to industrial applications than the flow-through configuration [1, 2]. Indeed the former allows large residence times, high conversions per pass, and uniform potential distributions if the electrodes are sufficiently long in the electrolyte flow direction and thin in the current flow direction. In previous studies [3–5] a few aspects of the application of nickel foams as materials for flow-by porous electrodes were considered. These studies were completed by a study of the electrode potential distribution in conditions of limiting current, i.e. of maximum productivity.

The first deductions of theoretical potential distributions in highly conductive flow-by porous electrodes operating in the diffusional regime were due to Alkire and Ng for a cylindrical geometry [2] and to Tentorio and Casolo-Ginelli for a parallelepipedic geometry [6]. By assuming that only the current density vector normal to the electrolyte flow has to be taken into account, they obtained simple analytical expressions giving the local electrode potential. The maximum potential drop is localized at the electrode entrance and it is considered as a design criterion, a

0021-891X/90 $03.00 + .12

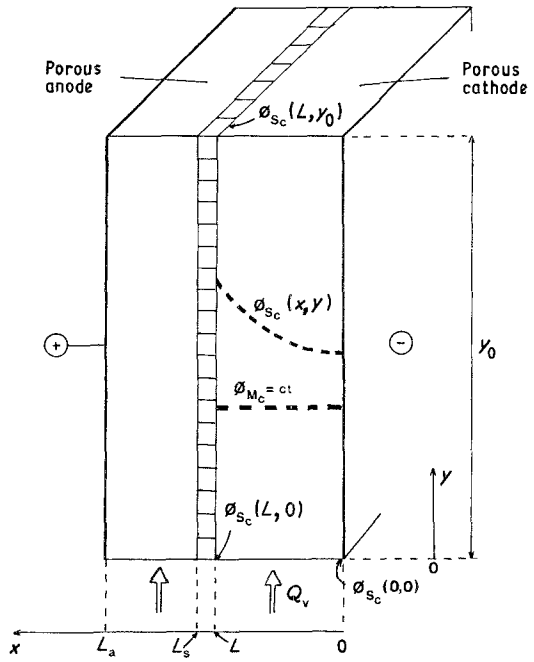

Fig. 1. Schematic view of the parallelepipedic cell.

conclusion which was confirmed by other approaches [7] and which led Kreysa [8] to propose an electrode of variable thickness.

In order to improve the design of flow-by porous electrodes, the 2-dimensional electrode potential distribution was investigated by two groups [9, 10] at almost the same time. The analytical expressions obtained are complex and it seems that a one-dimensional approach similar to that of Tentorio [6] could be sufficient for the design of long thin electrodes [9] and/or for small conversions per pass [11]. These analyses suppose that the separator plane is an equipotential surface, but recent works on 2-dimensional potential distributions in the whole cell volume, and considering particularly the ohmic drop through the interelectrode space, made these analyses questionable. These works are, respectively, those of Mowla *et al.* [12] for a cylindrical geometry, of Fleischman *et al.* [13] for a parallelepipedic geometry, and of Fedkiw *et al.* [14] for an electrode of variable thickness. Unfortunately, as the mathematical solutions are numerical, the influence of the different parameters on the potential distribution is not explicit, thus analytical models are preferred in spite of the necessary approximations.

The present paper concerns a theoretical approach to the electrode potential distribution in flow-by porous electrodes, the geometry of which could be that of electrodes constructed with metallic foams. Analytical models which take into account the polarization of the counter-electrode and the ohmic separator resistance are proposed. An approximate, simply expressed model is shown to be adequate for the behavioural description of electrodes constructed with stacked sheets of metallic foams.

2. Theoretical analysis for the diffusional regime

Let us consider the case of a cell containing two flow-by porous electrodes separated as shown in Fig. 1 (the presence of a separator is at least a hydrodynamical necessity in order to guarantee the percolation of each porous electrode by a given electrolyte flow). The problem is to investigate the potential distribution within the cathode working in limiting diffusion conditions. The porous electrode matrix is assumed to be equipotential (metal potential ϕ_M = constant).

Most of the theoretical models [2, 6, 9, 10] suppose that the separator plane ($x = L$) is at a constant solution potential, ϕ_S, a situation which neglects the ohmic drop of the interelectrode space but also admits the equipotentiality of the counter-electrode. This anode equipotentiality may be obtained with anodic gas evolution and/or when the anode penetration by the current lines is very small (highly concentrated anolyte, very rapid anodic reaction, porous electrode of large specific surface area). It seems that only Fedkiw [9] examined, in a simple manner, the influence of the ohmic resistance of the interelectrode space on the potential distribution within porous electrodes.

2.1. *Potential distribution in the cell*

The solution potential, ϕ_S, in a porous electrode follows from the differential charge balance [6, 9, 10, 15]:

$$\nabla^2 \phi_S = -\frac{a_e}{\gamma} i_R \qquad (1)$$

where a_e is the specific electrode surface area (per unit volume of electrode), i_R the local reaction current density and γ the apparent electrolyte conductivity in the pores of the electrode matrix. For a diffusion controlled simple cathodic reaction with z electrons, i_R is related to the mean mass transfer coefficient, $\bar{k}_d$, (assuming that the local mass transfer coefficient does not depend on the position and is equal to the mean value $\bar{k}_d$), as:

$$i_R = -zF\bar{k}_d C \qquad (2)$$

where C represents the local concentration of the reacting ions. If plug flow can be assumed in the porous electrode (no axial dispersion), the concentration only varies in the y direction of the electrolyte flow. That is:

$$C(y) = C_0 \exp[-\bar{k}_d a_e y/\bar{u}] \qquad (3)$$

where C_0 is the value of C at the electrode entrance ($y = 0$) and $\bar{u}$ is the mean electrolyte flow velocity based on the empty cross-sectional area. Thus, the Poisson Equation 1, giving the cathodic solution potential, ϕ_{S_c}, follows from (2) and (3):

$$\nabla^2 \phi_{S_c} = \frac{zF\bar{k}_d a_e C_0}{\gamma_c} \exp[-\bar{k}_d a_e y/\bar{u}] \qquad (4a)$$

In parallelepipedic flow-by porous electrodes, ϕ_{S_c} may vary with two coordinates x and y (2-dimensional problem) and solution of the following differential

equation becomes necessary:

$$\frac{\partial^2 \phi_{S_c}}{\partial x^2} + \frac{\partial^2 \phi_{S_c}}{\partial y^2} = \alpha \exp(-\beta y) \quad (4b)$$

with

$$\alpha = \frac{zF\bar{k}_d a_e C_0}{\gamma_c} \quad \text{and} \quad \beta = \frac{\bar{k}_d a_e}{\bar{u}}$$

The continuity of the solution potential and of the current density at the boundary between the different parts of the cell means that the anodic polarization and the ohmic resistance of the separator influence the distribution of ϕ_{S_c}. The distributions of the corresponding solution potentials ϕ_{S_c} and ϕ_{S_a} are respectively given by:

in the separator

$$\frac{\partial^2 \phi_{S_s}}{\partial x^2} + \frac{\partial^2 \phi_{S_s}}{\partial y^2} = 0 \quad (5)$$

in the porous anode

$$\frac{\partial^2 \phi_{S_a}}{\partial x^2} + \frac{\partial^2 \phi_{S_a}}{\partial y^2} = -\frac{a_{ea}}{\gamma_a} i_a \quad (6)$$

where a_{ea}, i_a and γ_a are the values of a_e, i_R, and γ for the anode.

The simultaneous solution of (4b), (5) and (6) leads to the distribution of ϕ_S in the cell, but the polarization law of the anode (i.e. the relation between ϕ_{S_a} and i_a) has to be known previously. Both cases of a small polarization of the anode and that of an equipotential anode have been considered.

2.2. *Case of a small anodic polarization*

Near the equilibrium potential the following linear approximation applies:

$$i_a(x, y) = \frac{zF}{RT} i_{oa}(x, y) \times \eta_a(x, y) \quad (7)$$

where i_{oa} is the anodic exchange current density, and $\eta_a = E_a - E_{oa}$ is the overpotential. As the anodic polarization is small, the anolyte conversion through the anode is also small, thus i_{oa} and the equilibrium potential, E_{oa}, can be considered as constant throughout the anode volume. If the anode matrix is equipotential (potential ϕ_{M_a} = constant), the introduction of the anodic solution potential, ϕ_{S_a}, in (7) leads to

$$i_a(x, y) = -\frac{zF}{RT} i_{oa}[\phi_{S_a}(x, y) - V] \quad (8)$$

where V is a constant which represents the difference $\phi_{M_a} - E_{oa}$.

The solution potentials ϕ_{S_a}, ϕ_{S_s} and ϕ_{S_c} in the three elements of the cell are obtained from the following differential equations, respectively:

in the anode ($L_s < x < L_a$)

$$\nabla^2 \phi_{S_a} = K^2(\phi_{S_a} - V) \quad (9)$$

with

$$K^2 = \frac{a_{ea}}{\gamma_a} \frac{zF}{RT} i_{oa}$$

in the separator ($L < x < L_s$)

$$\nabla^2 \phi_{S_s} = 0 \quad (5)$$

in the cathode ($0 < x < L$)

$$\nabla^2 \phi_{S_c} = \alpha \exp(-\beta y) \quad (4)$$

The limiting conditions of the problem correspond to the following hypothesis:

– the walls of the cell are not conductive:

$$\left(\frac{\partial \phi_{S_a}}{\partial x}\right)_{x=L_a} = \left(\frac{\partial \phi_{S_c}}{\partial x}\right)_{x=0} = 0 \quad (10a)$$

– there is continuity of the solution potential and of the current density at the boundaries:

$$\phi_{S_a}(L_s, y) = \phi_{S_s}(L_s, y) \quad (10b)$$

$$\phi_{S_s}(L, y) = \phi_{S_c}(L, y) \quad (10c)$$

for the solution potential and:

$$-\gamma_a \left(\frac{\partial \phi_{S_a}}{\partial x}\right)_{x=L_s} = -\gamma_s \left(\frac{\partial \phi_{S_s}}{\partial x}\right)_{x=L_s} \quad (10d)$$

$$-\gamma_c \left(\frac{\partial \phi_{S_c}}{\partial x}\right)_{x=L} = -\gamma_s \left(\frac{\partial \phi_{S_s}}{\partial x}\right)_{x=L} \quad (10e)$$

for the current density.

– the two porous electrodes (anode and cathode) have the same length y_0, they are exactly in front of each other, and there is no loss of current out of the three elements at the limits $y = 0$ and $y = y_0$:

$$\left(\frac{\partial \phi_S}{\partial y}\right)_{y=0} = \left(\frac{\partial \phi_S}{\partial y}\right)_{y=y_0} = 0 \quad \text{for} \quad 0 \leqslant x \leqslant L_a \quad (10f)$$

As in [11] the solution of Equations 4, 5, 9 and 10 uses a cosinus Fourier transformation and leads to the following analytical expression for $\phi_{S_c}(x, y)$:

$$\phi_{S_c}(x, y) = V + \frac{\alpha}{\beta y_0}(1 - e^{-\beta y_0})\left[\frac{x^2 - L^2}{2} - \gamma_c L \frac{(L_s - L)}{\gamma_s} - \left(\frac{\gamma_c}{\gamma_a}\right)\left(\frac{L}{K}\right)\coth[K(L_a - L_s)]\right]$$

$$+ 2\frac{\alpha\beta}{y_0}\sum_{n=1}^{\infty}\frac{1 - (-1)^n e^{-\beta y_0}}{\lambda^2(\lambda^2 + \beta^2)}\cos(\lambda y)$$

$$\left[\frac{\operatorname{ch}(\lambda x)}{\operatorname{ch}(\lambda L) + \frac{\gamma_c}{\gamma_s}\operatorname{sh}(\lambda L)\operatorname{th}[\lambda(L_s - L)]\dfrac{\gamma_a \mu \operatorname{th}[\mu(L_a - L_s)] + \gamma_s \lambda \coth[\lambda(L_s - L)]}{\gamma_a \mu \operatorname{th}[\mu(L_a - L_s)] + \gamma_s \lambda \operatorname{th}[\lambda(L_s - L)]}} - 1\right] \quad (11a)$$

with

$$\lambda = n\pi/y_0 \quad \text{and} \quad \mu = \lambda + K.$$

An approximate expression is easily obtained for ϕ_{S_c} if it is supposed that the thickness of each cell element is small, thus neglecting the y derivate in Equations 4, 5 and 9. This expression is:

$$\phi_{S_c}(x, y) - V = \alpha\, e^{-\beta y}\left[\frac{x^2 - L^2}{2} - \gamma_c L\frac{(L_s - L)}{\gamma_s} - \left(\frac{\gamma_c}{\gamma_a}\right)\left(\frac{L}{K}\right)\coth\left[K(L_a - L_s)\right]\right] \tag{11b}$$

2.3. *Case of an equipotential anode*

If the polarization of the anode is negligible and/or if only a very small fraction of the anode volume is electrochemically active (small effectiveness) and/or if gas is evolved at the anode, the equipotentiality of the anodic separator side can be assumed:

$$\phi_{S_a}(L_s, y) = \text{constant}$$

Then, the solution of Equations 4, 5, 10 by means of a cosinus Fourier transformation leads to the following rigorous expression of the solution potential within the cathode volume:

$$\phi_{S_c}(x, y) = V + \frac{\alpha}{\beta y_0}(1 - e^{-\beta y_0})\times\left[\frac{x^2 - L^2}{2} - \left(\frac{\gamma_c}{\gamma_s}\right)L(L_s - L)\right] + 2\frac{\alpha\beta}{y_0}\sum_{n=1}^{\infty}\frac{1 - (-1)^n e^{-\beta y_0}}{\lambda^2(\lambda^2 + \beta^2)}\times\left[\frac{\text{ch}(\lambda x)}{\text{ch}(\lambda L) + \frac{\gamma_c}{\gamma_s}\text{sh}(\lambda L)\,\text{th}\left[\lambda(L_s - L)\right]} - 1\right]\cos(\lambda y) \tag{12a}$$

with

$$\lambda = n\pi/y_0 \quad \text{and} \quad V = \phi_{S_s}(L_s, y).$$

As previously, an approximate solution can be obtained neglecting the terms $\partial^2\phi_s/\partial y^2$ in Equations 4 and 5:

$$\phi_{S_c}(x, y) - V = \alpha\, e^{-\beta y}\left[\frac{x^2 - L^2}{2} - \frac{\gamma_c}{\gamma_s}L(L_s - L)\right] \tag{12b}$$

The ratio $(L_s - L)/\gamma_s$ represents the specific separator resistivity r_s. Thus expression (12b) can also be applied to the case of ion exchange membranes of small thickness. This expression was first proposed by Fedkiw [9] who considered a cell containing a porous cathode, a planar anode and in which the anolyte occupied the interelectrode space.

2.4. *Existing analytical models*

The models proposed by Fedkiw [9], Storck [10] and Tentorio [6] suppose that the counter-electrode polarization and the ohmic drop through the inter-electrode space are negligible. Thus they assume that the solution potential $\phi_{S_c}(L, y)$ at the boundary between the separator and the porous electrode is independent of y.

The solution obtained from Equation 4 in [10] is:

$$\phi_{S_c}(x, y) = \phi_{S_c}(L, y) + \frac{\alpha}{\beta y_0}(1 - e^{-\beta y_0})\frac{x^2 - L^2}{2} + 2\frac{\alpha\beta}{y_0}\sum_{n=1}^{\infty}\frac{1 - (-1)^n e^{-\beta y_0}}{(\beta^2 + \lambda^2)\lambda^2}\left[\frac{\text{ch}(\lambda x)}{\text{ch}(\lambda L)} - 1\right]\cos(\lambda y) \tag{13a}$$

This expression was experimentally checked in [10] for the case of fixed bed electrodes of spheres (bed porosity nearly 0.4). The solution deduced by Fedkiw [9] agrees sufficiently well with (13a) when the conversion per pass is higher than 30% and for geometrical ratio, y_0/L, smaller than 20.

When the converson per pass is small [11] and/or when the electrode geometrical ratio, y_0/L, is high [9], the potential change along the electrode height is small and, thus, $\partial^2\phi_{S_c}/\partial y^2$ can be neglected in Equation 4. Thus, the following approximate solution, first obtained by Tentorio [6], is deduced:

$$\phi_{S_c}(x, y) - V = \alpha\, e^{-\beta y}\left(\frac{x^2 - L^2}{2}\right) \tag{13b}$$

Expression (13b) was in agreement with the experimental results of Leroux [16] concerning flow-by electrodes constructed with expanded metal (porosity of about 0.8).

2.5. *Conclusions*

Table 1 summarizes the expressions obtained with the different models. Except for the sign and index, these expressions also apply to flow-by porous anodes. As the models suppose a small or negligible polarization of the counter-electrode, they are independent of the compared electrolyte flow direction in the two cell compartments (co-current or counter-current flow).

It is interesting to note that in (11b), the solution potential, ϕ_{S_c}, results from three contributions which correspond respectively to:

– the potential change through the cathode thickness, by the factor $(x^2 - L^2)/(2\gamma_c)$

– the ohmic drop through the separator, by the factor $(L_S - L)/\gamma_s$

– the anode polarization, by the factor $(1/\gamma_a) \times 1/K \coth\left[K(L_a - L_s)\right]$

The approximate Equation 12b corresponds to the case where the above last contribution is negligible; the approximate Equation 13b follows by neglecting the above two last contributions. The sign of the terms

Table 1. Analytical expressions giving the solution potential distribution $\phi_{S_c}(x, y)$

1. *The plane $x = L$ is equipotential*

- Storck *et al.* [10]

$$\phi_{S_c}(x, y) = \phi_{S_c}(L, y) + \frac{\alpha}{\beta y_0}(1 - e^{-\beta y_0})\frac{x^2 - L^2}{2} + 2\frac{\alpha\beta}{y_0}\sum_{n=1}^{\infty}\frac{1 - (-1)^n e^{-\beta y_0}}{(\beta^2 + \lambda^2)\lambda^2}\left[\frac{\text{ch}(\lambda x)}{\text{ch}(\lambda L)} - 1\right]\cos(\lambda y) \quad (13a)$$

- Tentorio and Casolo-Ginelli [6]

$$\frac{\partial^2\phi_{S_c}}{\partial y^2} \ll \frac{\partial^2\phi_{S_c}}{\partial y^2}$$

$$\phi_{S_c}(x, y) - V = \alpha e^{-\beta y}\left(\frac{x^2 - L^2}{2}\right) \quad (13b)$$

2. *The plane $x = L$ is equipotential*

- Rigorous model

$$\phi_{S_c}(x, y) = V + \frac{\alpha}{\beta y_0}(1 - e^{-\beta y_0})\left[\frac{x^2 - L^2}{2} - \frac{\gamma_c}{\gamma_s}L(L_s - L)\right] + 2\frac{\alpha}{y_0}\sum_{n=1}^{\infty}\frac{1 - (-1)^n e^{-\beta y_0}}{\lambda^2(\lambda^2 + \beta^2)}$$

$$\times\left[\frac{\text{ch}(\lambda x)}{\text{ch}(\lambda L) + \frac{\gamma_c}{\gamma_s}\text{sh}(\lambda L)\,\text{th}[\lambda(L_s - L)]} - 1\right]\cos(\lambda y) \quad (12a)$$

- Approximate model

$$\frac{\partial^2\phi_{S_c}}{\partial y^2} \ll \frac{\partial^2\phi_{S_c}}{\partial x^2}$$

$$\phi_{S_c}(x, y) - V = \alpha e^{-\beta y}\left[\frac{x^2 - L^2}{2} - \frac{\gamma_c}{\gamma_s}L(L_s - L)\right] \quad (12b)$$

3. *Small anodic polarization*

- Rigorous model

$$\phi_{S_c}(x, y) = V + \frac{\alpha}{\beta y_0}(1 - e^{-\beta y_0})\left[\frac{x^2 - L^2}{2} - \gamma_c L\frac{(L_s - L)}{\gamma_s} - \frac{\gamma_c}{\gamma_a}\frac{L}{K}\coth[K(L_a - L_s)]\right] + 2\frac{\alpha\beta}{y_0}\sum_{n=1}^{\infty}\frac{1 - (-1)^n e^{-\beta y_0}}{\lambda^2(\lambda^2 + \beta^2)}\cos(\lambda y)$$

$$\times\left[\frac{\text{ch}(\lambda x)}{\text{ch}(\lambda L) + \frac{\gamma_c}{\gamma_s}\text{sh}(\lambda L)\,\text{th}[\lambda(L_s - L)]\frac{\gamma_a\mu\,\text{th}[\mu(L_a - L_s)] + \gamma_s\lambda\coth[\lambda(L_s - L)]}{\gamma_a\mu\,\text{th}[\mu(L_a - L_s)] + \gamma_s\lambda\,\text{th}[\lambda(L_s - L)]}} - 1\right] \quad (11a)$$

- Approximate model

$$\frac{\partial^2\Phi_{S_c}}{\partial y^2} \ll \frac{\partial^2\phi_{S_c}}{\partial x^2}$$

$$\phi_{S_c}(x, y) - V = \alpha e^{-\beta y}\left[\frac{x^2 - L^2}{2} - \gamma_c L\frac{(L_s - L)}{\gamma_s} - \frac{\gamma_c}{\gamma_a}\frac{L}{K}\coth[K(L_a - L_s)]\right] \quad (11b)$$

with

$$K = \left(\frac{a_{ea}}{\gamma_a}\frac{zF}{RT}i_{oa}\right)^{1/2}$$

in (11b) shows that the anode polarization and the ohmic separator resistance have a negative influence on the uniformity of the solution potential distribution within the porous cathode. In other words the uniformity of the potential distribution within the porous cathode is improved by reducing the above three contributions; this also makes the potential distribution in the other cell elements more uniform.

3. Application to the design of flow-by porous electrodes

3.1. *Presentation of the problem*

For any of the approximate models [Equation 11b; 12b or 13b], the solution potential drop (i.e. the electrode potential drop) through the thickness of the porous cathode is expressed as:

$$\Delta\phi_{S_c}(y) = \phi_{S_c}(L, y) - \phi_{S_c}(0, y) = \alpha e^{-\beta y}\frac{L^2}{2}$$

and is maximum at the entrance ($y = 0$). Thus, the separator resistivity and the anodic polarization only influence the longitudinal distribution of the solution potential in the porous cathode.

As seen in Fig. 1 the maximum solution potential drop in the cathode, $(\Delta\phi_{S_c})_{max}$, is then equal to the sum of the potential drop through the thickness at the entrance ($y = 0$) and of the potential drop all along the electrode length at the boundary with the separ-

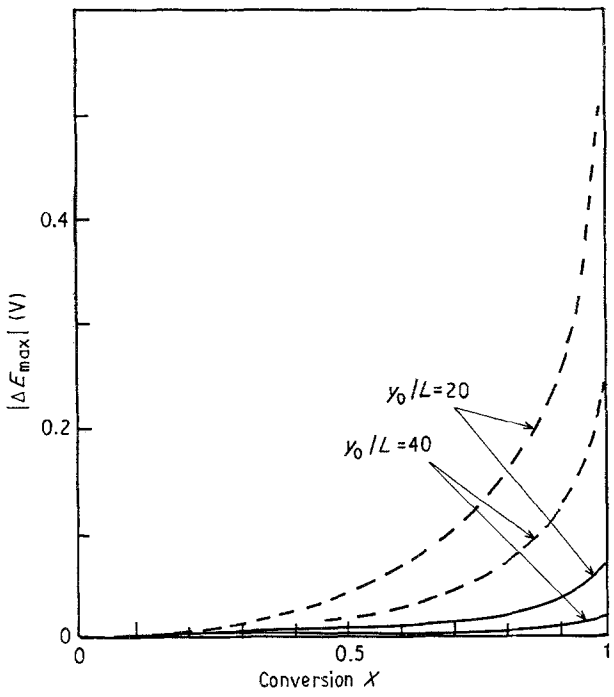

Fig. 2. Variation of the maximum potential drop with conversion. Parameters: $y_0 = 0.01$ m; $L_s - L = 4 \times 10^{-3}$ m; $\bar{u} = 0.01$ m s^{-1}; $z = 1$; $C_0 = 2.5$ mol m^{-3}; $\gamma_c = \gamma_0 = 20\,\Omega^{-1}$ m^{-1}; $\gamma_0/\gamma_s = 4$. Equation 12b (- - -); Equation 13b (——).

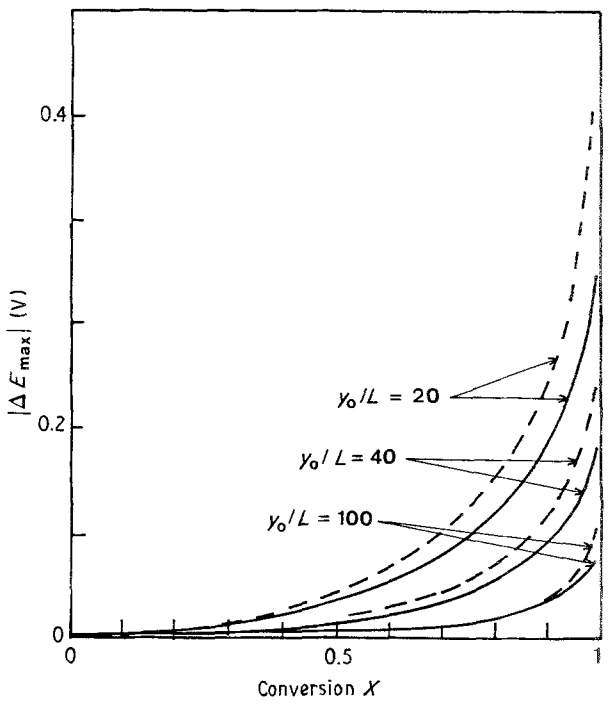

Fig. 3. Variation of the maximum potential drop with the conversion: comparison between the rigorous and the approximate models taking the separator influence into account. Same parameters as in Fig. 2. Equation 12a (——); Equation 12b (- - -).

ator ($x = L$), that is:

$$(\Delta\phi_{S_c})_{max} = [\phi_{S_c}(L, y_0) - \phi_{S_c}(L, 0)] + [\phi_{S_c}(L, 0) - \phi_{S_c}(0, 0)]$$

or

$$(\Delta\phi_{S_c})_{max} = \phi_{S_c}(L, y_0) - \phi_{S_c}(0, 0)$$

This solution potential drop $(\Delta\phi_{S_c})_{max}$ is equal, but with an opposite sign, to the maximum extent of the cathode potential $(\Delta E_c)_{max}$.

For a cathodic reaction, the more negative electrode potential $E_c(x, y)$ is at $y = y_0$ and near the separator ($x = L$); the less cathodic potential is situated at the electrode entrance ($y = 0$) and near the non-conducting cell wall ($x = 0$).

As the experimental cell used in the experiments [17] did not allow measurement of the counter-electrode (anode) potentials, the model which assumes a small anodic polarization could not be experimentally checked. This is the reason why, in view of [17], only the models which consider an equipotential counter-electrode will be compared below.

3.2. *Comparison of the maximum potential drops*

3.2.2. Influence of the separator. In order to illustrate the influence of the separator, the maximum potential drops, $(\Delta E_c)_{max}$, obtained using (12b) and (13b) were compared. Figure 2 shows such a comparison as a function of the conversion X, for two values of the geometrical ratio y_0/L of the porous cathode. These two values chosen for y_0/L correspond to those which were obtained with stacks of nickel foam (the foam exists in the form of sheets approximately 0.25 cm thick) located behind a ceramic separator 0.4 cm thick [17]. It is clear from Fig. 2 that the separator influence cannot be neglected *a priori*; in the present example, deviations reaching 500% are observed between (12b) and (13b) when X is higher than 0.6.

The comparison of Equations 12b and 13b shows indeed that the separator influence in the calculation of $(\Delta E)_{max}$ can only be neglected if:

$$\frac{L}{2\gamma_c} \gg X\frac{L_s - L}{\gamma_s} = Xr_s \qquad (15)$$

i.e., when:

– the conversion per pass X is small

– the separator is thinner than the porous electrode

– the porosity $\bar{\varepsilon}$ of the electrode is small [for a bed of spherical conducting grains ($\bar{\varepsilon} \sim 0.4$) the ratio γ_0/γ_c is nearly 3.5].

This agrees with the experimental results of Leroux [16] and Enriquez-Granados [12, 18] who showed that the solution potential near the separator boundary ($x = L$) was constant along the electrode height. With porous electrodes made of nickel foam (high porosity, thin electrodes), the separator influence cannot be neglected [17].

In Fig. 2 it is seen that the maximum potential drop increases rapidly with X; this is due to the exponential function existing in the plug flow model. Thus, when the maximum allowable electrode potential drop is a limiting factor, a single electrochemical reactor without recycling would not permit a high conversion.

3.2.3. Comparison of the models considering the influence of the separator. Figure 3 represents, as a function

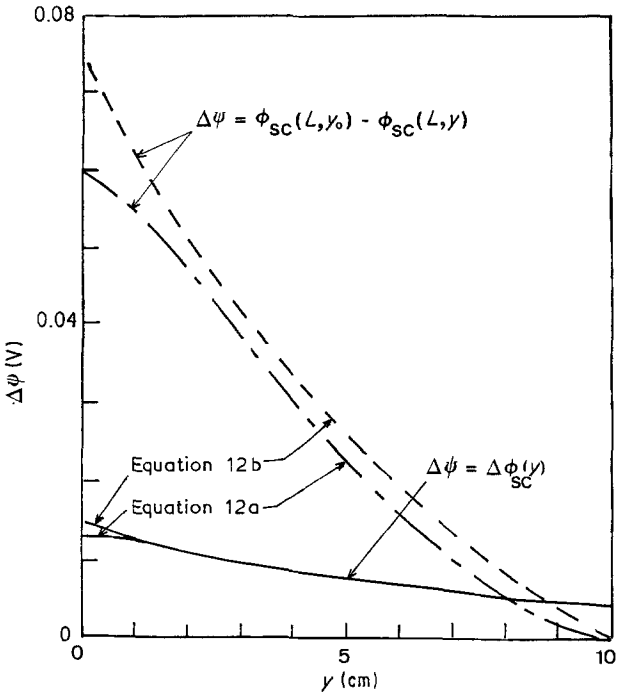

Fig. 4. Longitudinal distribution of ϕ_{S_c} and of the potential drop across the electrode thickness, calculated from the models which take the separator influence into account. Parameters: the same as in Figs 2–3 and $L = 0.0045$ m; $X = 0.75$.

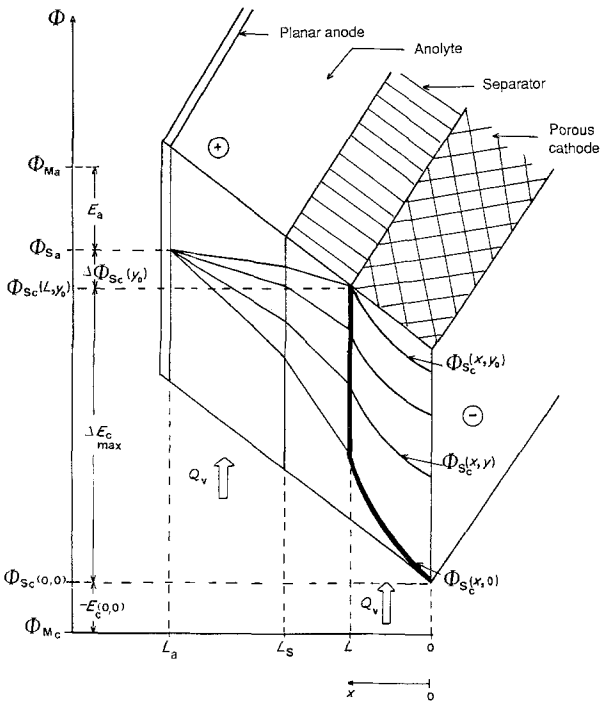

Fig. 5. Representation of the solution potential distribution across the cell thickness.

of X and for three values of y_0/L, the variations of $|\Delta E_{max}|$ deduced from (12a) and (12b). In Equation 12a, the Fourier series is calculated up to $n = 50$. The deviations between the rigorous (Equation 12a) and the approximate (Equation 12b) models increase when the conversion increases and/or when the geometrical ratio y_0/L decreases. As these deviations are smaller than 25%, Equation 12b could be seen as acceptable for high y_0/L values (case of metallic foam). Figure 4 shows longitudinal solution potential distributions in the plane $x = L$; these were calculated from Equations 12a and 12b for a stack of two sheets of 100 ppi (pores per inch) nickel foam. Figure 4 also shows the variations of the overall potential drop across the stack thickness, $\Delta\phi_{S_c}(y)$, with the longitudinal coordinate y. It is seen that the deviations between the models are essentially located at the electrode extremities. As Equation 12b is simple, it could be useful for the design of flow-by porous electrodes having a high geometrical ratio y_0/L and associated with an equipotential counter-electrode.

3.3. *Application to the design of flow-by porous electrodes*

Figure 5 shows schematically a two-compartment parallelepipedic cell which could be the unit element of a filter-press system. In this case a planar counter-electrode (anode) is assumed. The distributions of the solution potential across the cell thickness are represented according to the approximate model which neglects the anodic polarization.

In an industrial application, a given cell productivity per unit time is generally desired jointly with a high selectivity, in other words, avoiding secondary reactions. This selectivity depends on the extent of the electrode potential variation range, ΔE, one limit of which is the local electrode potential $E(0, 0)$. The potential $E(0, 0)$ may be fixed *a priori* on a thermodynamical and kinetic basis.

The specific productivity, P, represents the amount of matter formed (or produced) per unit time and volume of the porous electrode, that is:

$$P = Q_v \frac{C_0 - C_S}{V_R} = C_0 X \frac{\bar{u}}{y_0} \qquad (16)$$

where C_0 and C_S are the entrance and exit concentration respectively, $Q_v (= \bar{u} L \ell)$ is the flow-rate, and V_R is the electrode volume.

According to the approximate model [Equation 12b], the maximum electrode potential drop, $(\Delta E)_{max}$, is given by:

$$(\Delta E)_{max} = -zFC_0 \frac{\bar{u}L}{y_0} \ln(1 - X)\left[\frac{L}{2\gamma_c} + Xr_s\right] \qquad (12c)$$

As the electrode material and the separator are generally chosen *a priori*, then the minimum electrode volume $(L\ell y_0)$ which would be suited for the required production results from a compromise between the above expressions for P, Q_v and $(\Delta E)_{max}$ and mass transfer correlations such as those given in [5] for nickel foam electrodes. The above considerations essentially apply for limiting current conditions at any point of the electrode.

According to the Nernst equation, the equilibrium potential at y, where the concentration is $C(y)$, is expressed as:

$$E_{eq}(y) = E_0 + \frac{RT}{zF} \ln \frac{C(y)}{C_A}$$

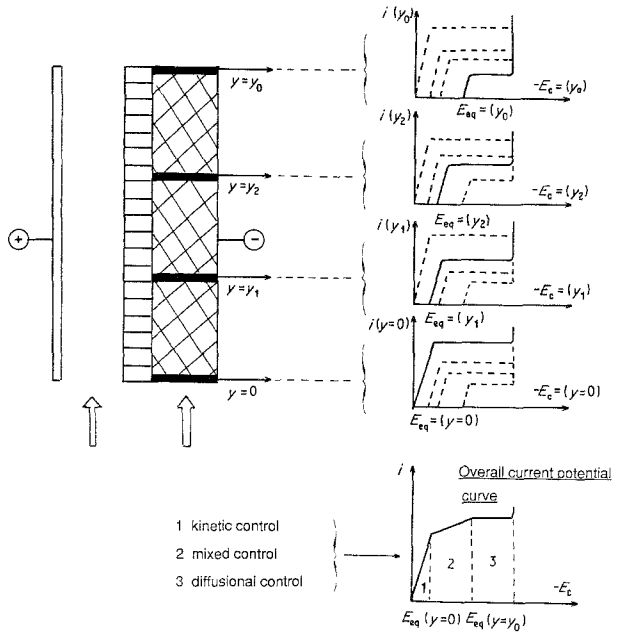

Fig. 6. Variation of the equilibrium potential E_{eq} along the electrode.

which becomes, assuming plug flow:

$$E_{eq}(y) = E_{eq}(y = 0) + \frac{RT}{zF} \ln (1 - X) \left(\frac{y}{y_0}\right)$$

Then the variation of E_{eq} along y may be significant.

Figure 6 shows the current density against the electrode potential curves which correspond to differential elements of electrode situated at different distances along this electrode. As indicated, the equilibrium potential varies along y. The zone of mixed control which appears in the overall curve is particularly interesting because:

– there is a one to one relation between current intensity and potential

– with respect to the electrolyte flow direction, the upward electrode region works in the kinetic control regime while the downward region works in limiting current conditions.

Such a mixed control was observed during experiments with nickel foam electrodes [17]; these seem well suited to industrial operating conditions if a high electrode productivity is required.

4. Conclusions

The comparison of theoretical models shows that the solution potential distribution within the porous electrode of a two-compartment cell depends greatly on the ohmic resistance of the separator, when the conversion per pass is high and/or when the thickness of the porous electrode is small. For flow-by porous electrodes made of thin porous materials (metallic foams, for example), the influence of the separator has to be taken into account. Up to conversion of about 90% the approximate model does not differ from the corresponding rigorous model, and thus can be usefully used for the design of flow-by porous electrodes working in conditions of high productivity and in cells such that the counter-electrode potential can be considered as constant. The use of the model leads to the porous electrode volume for a one-pass operation.

The cases of reactors in series and/or operating with recycle was not considered here in spite of the interest in such situations for the achievement of a uniform potential distribution and a high conversion. However the extension of the approximate model to such cases would not present mathematical difficulties.

Finally, it has to be noted in Equation 12b, which corresponds to the case of a small counter-electrode polarization, that the simultaneous operation of the two electrodes of the cell in conditions of high productivity has to be avoided. Indeed the polarization of each electrode influences the potential distribution in the other electrode. In the case where high conversions in the porous electrode would be needed, a counter-electrode working at constant potential would be recommended. The next paper [17], which reports experimental work on flow-by porous electrodes of nickel foam, confirms the present theoretical analysis.

References

[1] R. Alkire and P. K. Ng, *J. Electrochem. Soc.* **121** (1974) 95.
[2] *Idem, ibid.* **124** (1977) 1220.
[3] J. M. Marracino, F. Coeuret and S. Langlois, *Electrochim. Acta* **32** (1987) 1303.
[4] S. Langlois and F. Coeuret, *J. Applied Electrochem.* **19** (1989) 43.
[5] *Idem, ibid.* **19** (1989) 51.
[6] A. Tentorio and U. Casolo-Ginelli, *ibid.* **8** (1978) 195.
[7] M. Paulin, D. Hutin and F. Coeuret, *J. Electrochem. Soc.* **124** (1977) 180.
[8] G. Kreysa and C. Reynvaan, *J. Appl. Electrochem.* **12** (1982) 241.
[9] P. S. Fedkiw, *J. Electrochem. Soc.* **128** (1981) 831.
[10] A. Storck, M. A. Enriquez-Granados, M. Roger and F. Coeuret, *Electrochim. Acta* **27** (1982) 293.
[11] M. A. Enriquez-Granados, Thèse, I.N.P. de Nancy (1982).
[12] D. Mowla, H. Olive and G. Lacoste, *Electrochim. Acta* **28** (1983) 839.
[13] M. Fleischmann and R. E. W. Jansson, *ibid.* **27** (1982) 1029.
[14] P. S. Fedkiw and P Safemazandarini, *Chem. Eng. Comm.* **36** (1985) 27.
[15] F. Coeuret and A. Storck, 'Eléments de Génie Electrochimique', Tec-Doc Lavoisier, Paris (1984).
[16] F. Leroux and F. Coeuret, *Electrochim. Acta* **30** (1985) 167.
[17] S. Langlois and F. Coeuret, *J. Appl. Electrochem.* **20** (1990) 749.
[18] M. A. Enriquez-Granados, D. Hutin and A. Storck, *Electrochim. Acta* **27** (1982) 303.

Appendix

If ψ_s designates the difference $\phi_S - V = \phi_S - [\phi_{M_a} - E_{0a}]$, then the problem is to solve the following system of differential equations:

$$\left.\begin{aligned} \nabla^2\psi_{S_c} &= \alpha\, e^{-\beta y} \quad \text{for} \quad 0 < x < L \\ \nabla^2\psi_{S_s} &= 0 \qquad\qquad\quad L < x < L_s \\ \nabla^2\psi_{S_a} &= K^2\psi_{S_a} \qquad L_s < x < L_a \end{aligned}\right\} \quad \text{(A1)}$$

The cosinus Fourier transform is defined by:

$$\int_0^{y_0} \psi_S(x, y) \cos [n\pi y/y_0]\, dy = F(x, n)$$

$$\text{with} \quad n = 1, 2, 3, \ldots$$

$$F_a(x, n) = -\frac{C_1}{\lambda^2}\left[\frac{\text{ch}\,[\mu(L_a - x)]/\text{ch}\,[\lambda(L_s - L)]}{\text{ch}\left[\mu(L_a - L_s)\left(\coth(\lambda L)\,\text{th}\,[\lambda(L_s - L)] + \frac{\gamma_c}{\gamma_s}\right)\right.}\right.$$
$$\left.\left. + \frac{\gamma_a}{\gamma_s}\frac{\mu}{\lambda}\,\text{sh}\,[\mu(L_a - L_s)]\left(\coth(\lambda L) + \frac{\gamma_c}{\gamma_s}\,\text{th}\,[\lambda(L_s - L)]\right)\right]\right] \quad \text{(A4)}$$

Since

$$F\left(\frac{\partial^2\psi_S}{\partial y^2}\right) = (-1)^n\left(\frac{\partial\psi_S}{\partial y}\right)_{y=y_0} - \left(\frac{\partial\psi_S}{\partial y}\right)_{y=0} - \frac{n^2\pi^2}{y_0^2}F[\psi_S(x, y)]$$

the association of Equations A1 with the boundary conditions (Equation 10f) leads to the following system:

$$\begin{aligned}
\frac{d^2F_c(x, n)}{dx^2} - \lambda^2 F_c(x, n) &= \frac{\alpha\beta}{\beta^2 + \lambda^2}[1 - (-1)^n e^{-\beta y_0}] = C_1 \\
\frac{d^2F_s(x, n)}{dx^2} - \lambda^2 F_s(x, n) &= 0 \\
\frac{d^2F_a(x, n)}{dx^2} - \mu^2 F_a(x, n) &= 0
\end{aligned} \quad \text{(A2)}$$

with

$$\lambda = n\pi/y_0; \quad C_1 = [1 - (-1)^n e^{-\beta y_0}] \times \frac{\alpha\beta}{\beta^2 + \lambda^2} \quad \text{and} \quad \mu = K + \lambda$$

The general solution of (A2) is:

$$\left.\begin{aligned}
F_c(x, n) &= A_1 e^{-\lambda x} + B_1 e^{\lambda x} - C_1/\lambda^2 \\
F_s(x, n) &= A_2 e^{-\lambda x} + B_2 e^{\lambda x} \\
F_a(x, n) &= A_3 e^{-\mu x} + B_3 e^{\mu x}
\end{aligned}\right\} \quad \text{(A3)}$$

The coefficients $A_1, B_1, A_2, B_2, A_3, B_3$ are determined according to boundary conditions (Equations 10a to 10e).

Then it follows:

$$F_c(x, n) = \frac{C_1}{\lambda^2} \times \left[\frac{\text{ch}\,(\lambda x)}{\text{ch}\,(\lambda L) + \frac{\gamma_c}{\gamma_s}\,\text{sh}\,(\lambda L)\,\text{th}\,[\lambda(L_s - L)]Z} - 1\right]$$

$$F_s(x, n) = \frac{C_1}{\lambda^2} \times \left[\frac{\text{sh}\,[\lambda(L - x)] - \text{ch}\,[\lambda(L - x)]\,\text{th}\,[\lambda(L_s - L)]Z}{\frac{\gamma_s}{\gamma_c}\coth(\lambda L) + \text{th}\,[\lambda(L_s - L)]Z}\right]$$

with

$$Z = \frac{\gamma_a\mu\,\text{th}\,[\mu(L_a - L_s)] + \gamma_s\lambda\coth[\lambda(L_s - L)]}{\gamma_a\mu\,\text{th}\,[\mu(L_a - L_s)] + \gamma_s\lambda\,\text{th}\,[\lambda(L_s - L)]}$$

$$C_1 = \frac{\alpha\beta}{\beta^2 + \lambda^2}[1 - (-1)^n e^{-\beta y_0}]$$

$$\lambda = n\pi/y_0 \quad \text{and} \quad \mu = \lambda + K$$

The inverse Fourier transform is:

$$\psi_S(x, y) = \frac{1}{y_0}F(x, 0) + \frac{2}{y_0}\sum_1^\infty F(x, n)\cos(\lambda y) \quad \text{(A5)}$$

As

$$F(x, 0) = \lim_{\substack{n\to 0\\ \lambda\to 0}} F(x, n)$$

it follows that

$$F_c(x, 0) = (1 - e^{-\beta y_0})\frac{\alpha}{\beta}\left[\frac{x^2 - L^2}{2} - \frac{\gamma_c}{\gamma_s}L(L_s - L) - \frac{\gamma_c}{\gamma_a}\frac{L}{K}\coth[K(L_a - L_s]\right]$$

from which Equation 11a is deduced for the cathodic solution potential distribution.

In the more simple case where the anodic solution potential is constant at $x = L_s$ (see section 2.4), the solution using the cosinus Fourier transform is similar.

Acknowledgements

The authors wish to express their gratitude to the Direction des Études et Recherches d'Electricité de France for their financial support.